

The Torun catalogue of 6.7 GHz methanol masers*

M. Szymczak**, P. Wolak, A. Bartkiewicz, and K.M. Borkowski

Torun Centre for Astronomy, Nicolaus Copernicus University, Gagarina 11, 87-100 Torun, Poland

Received 2012 Apr 13, accepted 2012 May 2

Published online 2012 Jul 20

Key words catalogues – masers – radio lines: ISM – stars: formation

We report the observations of 289 methanol maser sources at 6.7 GHz obtained over a two month period with the Torun 32 m telescope. The data form a catalogue of all objects north of $\delta = -22^\circ$ brighter than 7.5 Jy in the peak emission. The positions of sub-arcsecond accuracy are updated for 76 % of the objects. We find that about one third of the sources show changes in the peak fluxes by a factor of two or more on time scales of 8.5–9.5 years.

© 2012 WILEY-VCH Verlag GmbH & Co. KGaA, Weinheim

1 Introduction

The class II methanol maser at 6668.519 MHz is one of the most spectacular manifestations of nascent or newly formed high-mass stars which are still embedded in their natal molecular clouds (Menten 1991). It is potentially powerful tool for investigating the environments of these objects and their distribution in the Galaxy. High-resolution imaging of the maser line enables precise measurements of proper motions and trigonometric parallaxes (e.g. Reid et al. 2009; Rygl et al. 2010).

Extensive targeted surveys of low angular resolution (a few arcmin) have resulted in a large number of detections toward IRAS selected ultra-compact HII regions (Schutte et al. 1993; van der Walt, Gaylard & MacLeod 1995; van der Walt et al. 1996; Walsh et al. 1997; Szymczak, Hrynek & Kus 2000), OH and H₂O masers (Caswell et al. 1995; Xu et al. 2008). No methanol masers were detected toward low-mass star formation sites (Minier et al. 2003). Unbiased methanol surveys of selected areas of the Galactic plane (Caswell 1996; Ellingsen et al. 1996; Szymczak et al. 2002; Pandian, Goldsmith & Deshpande 2007; Green et al. 2009, 2010; Caswell et al. 2010) proved very effective in detecting methanol sources where no clear indicators of high-mass star formation were previously known.

Majority of sources from single-dish surveys have no positions of sufficient accuracy for VLBI and multi-wavelength studies. Hence several sources have been observed with radio arrays to determine the position with a sub-arcsecond or higher accuracy (e.g. Walsh et al. 1998; Bartkiewicz et al. 2009; Caswell 2009; Cyganowski et al. 2009; Xu et al. 2009; Green et al. 2010). In many cases the data from untargeted surveys are homogeneous in sensitivity and resolutions (Ellingsen et al. 1996; Szymczak et al. 2002; Pan-

dian et al. 2007; Green et al. 2010) but they were taken at various occasions over 9–22 months. This means that they are not entirely appropriate for variability studies.

There are several catalogues of 6.7 GHz masers based solely on the data from the literature (Xu, Zheng & Jiang 2003; Malyshev & Sobolev 2003; Pestalozzi, Minier & Booth 2005) which have some value for statistical purposes. Generally they contain highly inhomogeneous data of diverse quality and commonly taken with various instruments at very different epochs. Presently, after the recent observations by Ellingsen (2007), Pandian et al. (2007), Xu et al. (2008), Caswell et al. (2009) and Green et al. (2010), more than 1000 sources are known. In this paper we present the catalogue data for a large sample of 6.7 GHz methanol masers of the northern sky which form a database free of the above mentioned shortcomings. It is currently used as a reference for ongoing scheme of flux monitoring with the Torun 32 m telescope. Here we show a preliminary result of the maser variability on time scales of 8–10 years, whereas a detailed statistical analysis of the objects in the catalogue is postponed to a future paper.

2 Data

2.1 Selection of sources

Most of the maser sources (~80 %) in our catalogue were extracted from the Torun 32 m telescope surveys of nearly 1400 IRAS colour-selected sources (Szymczak et al. 2000) and unbiased search of the Galactic plane from $l = 8^\circ$ to 90° , $|b| \leq 0^\circ.52$ of which only data for the strip of $20^\circ \leq l \leq 40^\circ$ were published (Szymczak et al. 2002).

Data for the longitude ranges of 8° – 20° and 40° – 90° were obtained between 2001 January and 2003 December using the same triangular grid and observational setup as reported in Szymczak et al. (2002). About 14 880 sky positions were sampled. A channel spacing in the spectra was

* Table A1 and Fig. B1 are available at the CDS via <http://cdsarc.u-strasbg.fr/cgi-bin/qcat?J/AN/333/634>

** Corresponding author: msz@astro.uni.torun.pl

0.04 km s^{-1} and the velocity coverage was $\pm 90 \text{ km s}^{-1}$. For the galactic longitudes of 8° – 20° and 40° – 90° the bandwidth was centred at the local standard of rest velocity of 40 and 0 km s^{-1} , respectively. A typical 3σ sensitivity was 1.6 Jy in both targeted and blind surveys. The flux calibration uncertainty was of the order of 15% and the radial velocity determination was accurate down to 0.4 km s^{-1} . 17 out of the 128 sources detected in the regions $8^\circ \leq l \leq 20^\circ$ and $40^\circ \leq l \leq 90^\circ$ and not catalogued before 2007 are referred in Table A1 as “Unpublished data from the Torun 32 m dish”. Their spectra and basic parameters were published in Green et al. (2010) and Pandian et al. (2007).

The selection of 237 sources from our original list was constrained by the latitude of the Torun antenna. We have also searched the literature for the 6.7 GHz methanol maser line observations available in the NASA Astrophysics Data System (ADS) up to 1 November, 2008 and found further 50 objects north of declination -22° . All of them and another two objects (Fujisawa et al. 2008, private communication) were added to the observed list.

2.2 Observations

A sample of 289 sources was observed with the Torun 32 m radio telescope in 2008 December and 2009 January. The half-power beam width was 5.5 at 6668.519 MHz . A dual-channel receiver was used to measure simultaneously two opposite circular polarizations. Typical system temperature was 40 K. The autocorrelator spectrometer was configured to obtain the spectra in a bandwidth of 4 MHz with channel spacing of 0.04 km s^{-1} . The spectra were taken in a frequency switching mode with about 30 min integration time. The observations were pointed on the target positions as given in the references of the first measurements.

The spectral line flux densities were continuously calibrated by measuring the receiver response to the signal from a noise diode of known temperature. The stability of the system was checked through continuum observations of 3C123 and Vir A assuming flux densities from Ott et al. (1994). The non-variable methanol source 32.745–0.076 (Caswell et al. 1995; Szymczak et al. 2011) was used as the secondary calibrator.

The data were reduced using the standard procedures. The spectra have a typical 3σ uncertainty of $\sim 0.6 \text{ Jy}$ after averaging both polarizations. Hanning smoothing was only applied to noisy spectra. The flux calibration uncertainty was estimated to be of the order of $\pm 15\%$. The accuracy of the velocity measurements with respect to the local standard of rest was better than 0.005 km s^{-1} .

3 Catalogue and atlas

A total of 284 objects detected are listed in Table A1. Each entry of the catalogue contains the following information. Column 1 gives the source name derived from its galactic

coordinates. Three significant decimal digits in each coordinate are given for the sources observed with interferometric arrays. Column 2 gives an alternative name of the source. Columns 3 and 4 give the 2000.0 right ascension and declination, respectively. Column 5 gives the velocity range of emission at the 3σ level, ΔV . Column 6 gives the velocity of peak flux, V_p . Columns 7 and 8 give the peak flux density, S_p and integrated flux density, S_i , respectively. Column 9 gives the reference for the first detection. Column 10 gives the reference for the coordinates. Remarks on the multiple sources unresolved with the beam and on possible confusion effect are given in Col. 11. Note that the coordinates of sources given in Table A1 are derived largely from the high angular resolution studies published after 2009 January when our observations were completed. However, the actual observations were pointed on the positions inferred from single dish measurements or the positions of infrared counterparts. In Sect. 4.2 we discuss the effect of position offset on the flux density estimates.

The spectra are shown in Fig. B1. In 33 of the plots the emission from neighbouring sources near the edge of the antenna beam is shown. In these blended spectra the velocity ranges of the principal and confused sources are marked and their names are given if possible. For several confused sources detailed comments and references are also given in the notes to Table A1.

3.1 Galactic distribution

The galactic distribution of 284 sources in the catalogue is shown in Fig. 1. For the galactic longitude higher than 50° the number of sources rapidly drops, being 19% of the sample. The distribution in the galactic latitude has a full width at half-maximum (FWHM) of $0^\circ 39'$. These results are fully consistent with the trends reported previously (Pestalozzi et al. 2005; Pandian & Goldsmith 2007). The data of high angular resolution (see notes in Table A1) imply that 25 sites in the sample are actually clusters of two or more sources not resolved or barely resolved with the 32 m telescope beam. A total number of sources in the clusters is at least 68. The mean angular size of the cluster is 1.5 ± 0.3 . All but one cluster lay in the inner Galaxy ($l < 50^\circ$) and their distribution in the latitude has a FWHM of $0^\circ 26'$. The extent of the emission from the clusters is usually less than 17 km s^{-1} . This suggests that the emission comes from a cluster rather than physically separated objects.

3.2 Line parameters

The extent of the emission ranges from 0.6 to 28.5 km s^{-1} and its average and median values are $7.5 \pm 0.3 \text{ km s}^{-1}$ and 6.8 km s^{-1} , respectively. These values are similar to those reported in deep unbiased studies (Green et al. 2010; Pandian et al. 2007). The 9.621+0.196 and 133.947+1.064 are the brightest sources in the catalogue with the peak flux density of 4357 and 3275 Jy, respectively. The median values of

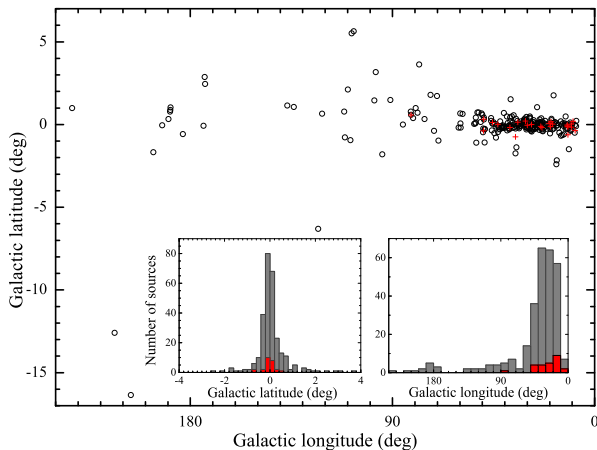


Fig. 1 (online colour at: www.an-journal.org) Distribution of the maser sources in the longitude-latitude plane. The crosses indicate the clusters of sources. The insets show histograms of objects versus the galactic longitude and galactic latitude. Histograms for the clusters (red colour) are overlaid.

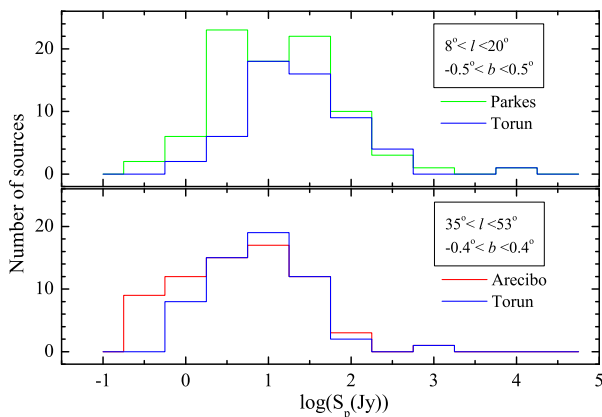


Fig. 2 (online colour at: www.an-journal.org) Histograms of the CH_3OH maser peak flux density for sources in the present sample and two comparison samples from untargeted surveys using the Parkes telescope (Green et al. 2010, *upper panel*) and the Arcibo telescope (Pandian et al. 2007, *lower panel*). The shared areas defined by the ranges of galactic coordinates are given in insets.

peak flux density and integrated flux density are 8.7 Jy and 10 Jy km s^{-1} , respectively.

4 Discussion

4.1 Completeness of catalogue

In order to examine the completeness of the catalogue we used the Parkes and Arcibo untargeted surveys (Green et al. 2010; Pandian et al. 2007). The Parkes telescope observed the region $8^\circ \leq l \leq 20^\circ$, $|b| \leq 2^\circ$ with a 3σ limit of 0.51 Jy and spectral resolution of 0.11 km s^{-1} (Green et al. 2010). In common strip of $8^\circ \leq l \leq 20^\circ$, $|b| \leq 0^\circ 52'$, 56 sources were found in the Torun untargeted survey with a detection threshold of 1.6 Jy , whereas with the Parkes

telescope 100 objects were detected. 25 out of those 100 sources formed clusters (2–3 sources) of average size less than $2/3$ and they could not be well resolved with the 32 m antenna. Therefore, 86 sources were used to compare with the Torun subsample obtained with smaller angular resolution. The median values of the peak flux density of sources in the Parkes and Torun subsamples were 5.7 and 10.6 Jy , respectively. The peak flux density of objects not detected in the Torun survey ranged from 0.2 to 12 Jy and the median value was 1.9 Jy . The strongest undetected source $9.215-0.202$ had $S_p = 11.9 \text{ Jy}$ in the pointed Parkes observations. Figure 2 (upper panel) shows the histograms of the peak flux density for both subsamples. Despite possible effect of variability (Sect. 4.3), it suggests that all the sources of $S_p > 7.6 \text{ Jy}$ within this surveyed area are included in our catalogue. This is slightly worse than the completeness limit of 5.2 Jy estimated for 20° to 40° longitude survey (Szymczak et al. 2002).

The Arcibo telescope surveyed the region $35^\circ 2' \leq l \leq 53^\circ 7'$, $|b| \leq 0^\circ 41'$ with a survey threshold of 0.27 Jy , spectral resolution of 0.14 km s^{-1} and the beam of $40''$ (Pandian et al. 2007). As the Arcibo survey had angular resolution a factor of 8.2 higher than that of the Torun survey we could resolve with the 32 m telescope only 69 of their 86 sources. In this region we catalogued 57 masers. Comparison of the flux density distribution in the two subsamples (Fig. 2, lower panel) indicates that the catalogue contains all the masers with $S_p > 1.8 \text{ Jy}$ detected in the Arcibo survey. This simply resulted from the inclusion of sources with S_p below the sensitivity (1.6 Jy) of our previous surveys but detected in the present observation. We conclude that the completeness of the catalogue is not uniform for the galactic longitude. Nevertheless, all maser sources brighter than 7.5 Jy in the peak are included.

4.2 Effect of pointing errors

The observations were pointed at the positions determined in the original targeted and blind surveys (Szymczak et al. 2000, 2002), which were accurate to about $0.5'$ for the signal to noise ratio higher than 10 and less than $1'$ for faint objects. Several methanol maser studies of different levels of astrometric accuracy were published after 2009 January (Bartkiewicz et al. 2009; Caswell 2009; Cyganowski et al. 2009; Green et al. 2010; Rygl et al. 2010; Xu et al. 2009) when data presented here were being gathered. There are 216 sources in the catalogue whose positions are known with an accuracy better than $1''$. Figure 3 shows the distribution of objects versus the angular separation between the position observed with the 32 m dish and that derived from astrometric measurements. The mean separation is 0.37 ± 0.04 and the median is 0.17 . Using the antenna beam pattern we estimate that in 94.9% (206/216) of the sources the position offset causes underestimation of the flux density by less than 10% that is comparable with the accuracy of flux calibration achieved in the present study. There are only 8 sources

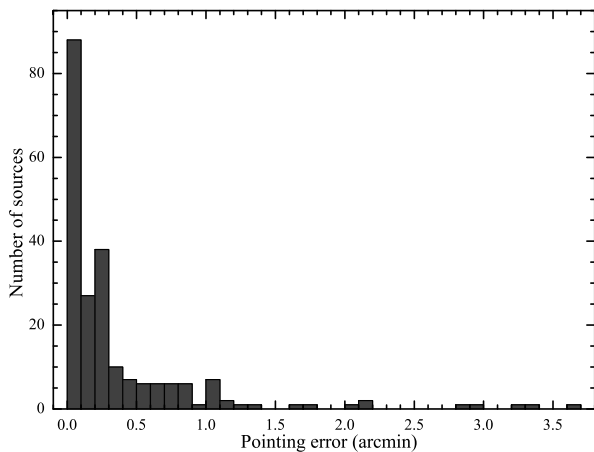


Fig. 3 Number of methanol masers as a function of angular offset between the astrometric and observed positions.

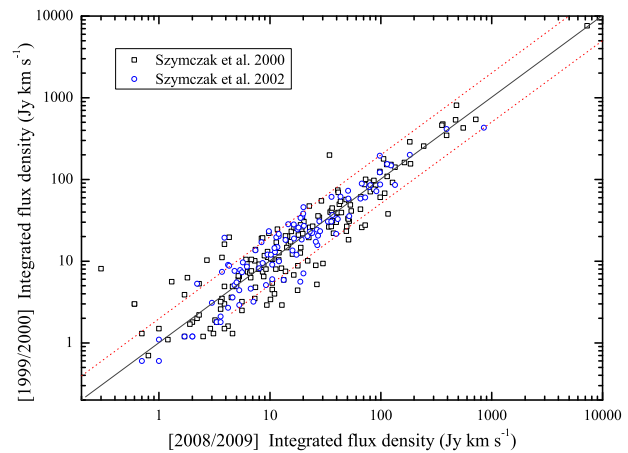


Fig. 5 (online colour at: www.an-journal.org) Same as in Fig. 4 but for the integrated flux density.

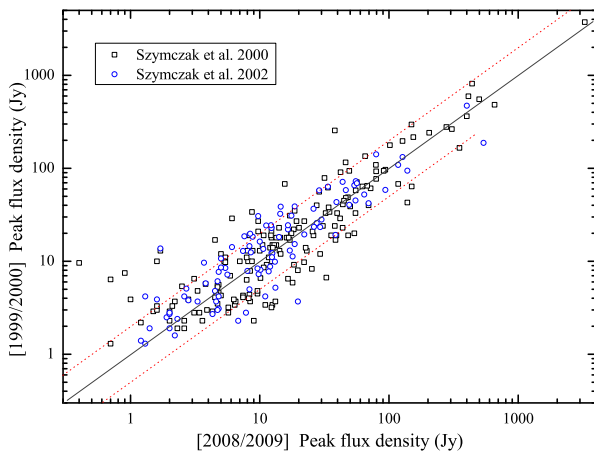


Fig. 4 (online colour at: www.an-journal.org) Variability in source peak flux density between the epoch 1999/2000 (Szymczak et al. 2000; Szymczak et al. 2002) and the present observations (epoch 2008/2009). The straight solid line corresponds to equal fluxes, whereas the dashed lines delimit the variability of 50%.

whose flux density is underestimated by about 50%. All those objects are indicated in Table A1.

4.3 Variability

A majority of sources in the catalogue were first observed from 1999 January to August (E1) (Szymczak et al. 2000) and between 2000 February and October (Szymczak et al. 2002), while the observations reported here were carried out from 2008 December to 2009 January (E2). Thus, we can determine a level of variability on time scales in the range 8.5 to 9.5 years. There are 204 sources in the sample for which we have the methanol spectra taken at both epochs.

Figure 4 shows the peak flux density at epoch 1999/2000 versus that at epoch 2008/2009. The flux density values group well around the equal flux density line with a scatter caused by the variability. The ratio of peak flux density at the first epoch to that at the second epoch observations has

the mean value of 1.12 ± 0.06 . There is a wider spread of flux density for weaker sources than for stronger ones. Very likely, it is the effect of relatively larger noise variations.

Comparison of the integrated flux densities at the two epochs is shown in Fig. 5. The mean value and dispersion for the ratio of integrated flux density at the first and second epochs are 1.21 and 0.05, respectively. This dispersion is slightly less than that seen for the peak flux density.

We find that the peak flux or integrated flux densities changed by a factor of two or more in 68 sources (Table 1); 37 sources increasing and 31 sources decreasing. Our fraction of highly variable sources 33.3% (68/204) is very similar to 31.5% deduced from a sample of 54 objects monitored over a period of ~ 4 years (Goedhart, Gaylard & van der Walt 2004), assuming that the highly variable sources have their variability index higher than 5. We notice different types of variability in our sample. For instance, the source 23.32–0.30 exhibited a strong decrease of the peak flux while the integrated flux density increased by a factor of 2.6. The peak flux density and the integrated flux density in the source 22.435–0.169 increased by factors of 3.8 and 5.1, respectively, while in the source 23.82+0.38 they decreased 2.4 and 2.7 times, respectively. A detailed investigation of individual strongly varying sources will be presented elsewhere.

High angular resolution studies of 6.7 GHz methanol masers indicate that individual spots show significant variability. For instance in the source 23.010–0.411 about 37% of the methanol spots change their brightness by more than 50%, whereas 83% of the total spots persist on time scale of two years (Sanna et al. 2010). Further VLBI observations will be useful to understand better the properties and origin of the variability. The present catalogue can serve as a guide to select the most interesting targets.

Comparison of our old and new data reveals the disappearance of five sources (Table 2). All of them were faint ($S_p < 6$ Jy) at the first epoch and were not re-detected with a 3σ sensitivity of 0.55–0.65 Jy at the second epoch. This sug-

Table 1 Highly variable sources.

Name	S_p (E1) (Jy)	S_p (E2) (Jy)	S_i (E1) (Jy km s ⁻¹)	S_i (E2) (Jy km s ⁻¹)	Name	S_p (E1) (Jy)	S_p (E2) (Jy)	S_i (E1) (Jy km s ⁻¹)	S_i (E2) (Jy km s ⁻¹)
10.444−0.018	9.8	22.0	23.3	48.8	30.317+0.070	11.0	5.4	19.0	8.4
10.629−0.333	3.4	6.4	2.9	12.8	30.701−0.064	43.0	138.6	27.7	72.2
10.886+0.123	4.5	9.6	8.2	12.7	30.790+0.205	19.8 ^a	8.4	45.9 ^a	20.1
11.497−1.485	116.0	46.2	178.8	105.7	30.816−0.052	4.3	7.4	4.4	17.8
12.904−0.031	8.3	25.3	9.4	30.1	30.97−0.14	5.9	17.9	8.9	25.9
13.179+0.061	6.4	0.7	3.0	0.6	31.064+0.093	6.5	16.5	4.0	11.0
13.713−0.083	3.4	12.5	3.5	7.3	32.992+0.034	27.0	9.7	22.0	9.8
14.101+0.087	135.0	65.3	152.3	112.9	34.751−0.093	9.7 ^a	3.7	9.0 ^a	4.2
14.604+0.017	2.9	1.5	5.3	2.3	35.197−0.743	64.0	150.	91.8	127.8
15.034−0.677	19.0	48.2	8.8	17.9	36.115+0.552	19.0	39.2	32.7	51.0
17.021−2.403	3.7	6.5	2.9	9.4	37.030−0.039	7.3 ^a	9.8	7.1 ^a	20.1
18.874+0.053	3.7	8.4	1.6	4.2	37.54−0.11	5.7	3.8	19.7	4.3
19.365−0.030	6.7	32.7	10.1	21.9	37.598+0.425	24.3 ^a	11.2	28.3 ^a	14.6
19.884−0.534	2.3	9.0	1.3	4.6	38.038−0.300	18.6 ^a	7.6	21.6 ^a	12.0
21.407−0.254	3.7	13.2	5.9	13.3	38.92−0.36	5.4	2.5	3.9	1.7
22.357+0.066	12.0	14.5	6.8	16.4	41.23−0.20	3.2	5.7	3.4	10.1
22.435−0.169	3.2	12.3	5.2	26.5	43.796−0.127	79.0	31.6	54.7	29.1
23.010−0.411	188.5 ^a	538.	431.3 ^a	849.9	43.890−0.784	34.0	8.7	25.5	17.3
23.207−0.377	12.0	29.3	43.4	65.6	50.01+0.59	6.5	3.1	6.6	5.2
23.257−0.241	4.4	8.3	4.5	10.5	53.04+0.11	3.3	1.6	1.3	0.7
23.32−0.30	2.2	1.2	1.5	3.9	58.77+0.64	2.8	5.7	4.8	7.4
23.389+0.185	17.0	38.5	31.0	52.0	60.57−0.19	4.1	7.4	1.2	2.5
23.481+0.092	12.0	5.0	9.2	8.0	73.06+1.80	10.0	1.6	6.3	1.8
23.82+0.38	9.6	0.4	8.1	0.3	78.122+3.633	38.0	34.1	18.3	51.1
24.493−0.039	29.0	6.1	24.6	11.7	108.184+5.519	91.0	42.1	47.4	22.6
24.68−0.16	3.5	4.7	2.5	5.6	108.76−0.95	2.8	3.4	1.3	3.1
24.850+0.087	13.0	1.7	16.1	3.9	111.26−0.77	4.0	8.2	6.5	8.8
25.411+0.105	8.0	19.7	12.6	18.8	136.84+1.15	21.0	9.7	11.1	3.7
25.80−0.16	20.0	53.9	26.0	67.3	173.482+2.446	256.0	38.1	198.6	34.5
26.61−0.21	19.0	8.3	20.4	13.8	173.69+2.88	7.5	0.9	3.0	0.6
27.220+0.260	2.8 ^a	7.8	3.2 ^a	7.1	183.35−0.58	18.0	13.4	19.3	8.6
28.39+0.08	3.4	11.0	8.0	9.2	189.77+0.34	17.0	4.5	10.3	2.7
28.70+0.40	4.2 ^a	1.3	0.6 ^a	0.7	196.454−1.677	68.0	15.6	37.9	116.0
30.30−0.20	3.9	1.0	5.6	1.3	213.705−12.597	166.0	350.4	155.7	184.9

^a Szymczak et al. (2002).**Table 2** Disappeared and appeared maser sources.

Name	Other Name	First Epoch S_p (Jy) [S_i (Jy km s ⁻¹)]	Second Epoch S_p (Jy) [S_i (Jy km s ⁻¹)]
14.44−0.06	IRAS18141−1626	3.0 [1.0]	<0.65 [<0.2]
15.08−0.12	IRAS18155−1554	3.1 [1.1]	<0.60 [<0.2]
26.64+0.02	IRAS18372−0537	5.9 [2.5]	<0.60 [<0.2]
30.59−0.13		2.2 [0.7]	<0.55 [<0.2]
43.18−0.52	IRAS19097+0847	5.5 [3.1]	<0.60 [<0.2]
52.23+0.73	IRAS19227+1721 ^a	<1.8 [<0.5]	4.2 [2.9]
107.29+5.64	IRAS22198+6336 ^a	<1.9 [<0.5]	1.5 [0.9]

^a Fujisawa et al. (2008, private communication).

gests that only $\sim 2\%$ of sources in the original sample disappeared after 9.5 years. We note that two sources (Table 2) in the catalogue were detected by Fujisawa et al. (2008, private communication) who re-observed the non-detections of the Szymczak et al. (2000) survey.

5 Summary

The paper presents observations of the 6.7 GHz methanol maser emission towards 289 targets. 284 sources were detected of which 25 sources form clusters unresolved with the 5.5 beam. A comparison of an earlier epoch data and the present survey reveals that 33% of the sources show significant variability (more than 50%) on time scale of 8.5 or 9.5 years. The catalogue can be the potential to become a reference for further studies of variability. Since the catalogue gives the interferometric position for about 76% of the sources it will be useful database for future VLBI measurements of the proper motions and trigonometric parallaxes.

Acknowledgements. We thank G. Fuller for communicating the MERLIN astrometric observations prior to publication, K. Fujisawa and K. Sugiyama for allowing us to use their methanol maser data observed with the Yamaguchi 32 m radio telescope before publication. We have made use of NASA's Astrophysics Data System Bibliographic Services and the SIMBAD database operated at CDS, Strasbourg, France. The work was supported by the Polish Ministry of Science and Higher Education through grant N N203 386937.

References

- Bartkiewicz, A., Szymczak, M., van Langevelde, H.J., Richards, A.M.S., Pihlström, Y.M.: 2009, *A&A* 502, 155
- Caswell, J.L.: 1996, *MNRAS* 279, 79
- Caswell, J.L.: 2009, *PASA* 26, 454
- Caswell, J.L., Vaile, R., Ellingsen, S., Whiteoak, J., Norris, R.: 1995, *MNRAS* 272, 96
- Caswell, J.L., Fuller, G.A., Green, J.A., et al.: 2010, *MNRAS* 404, 1029
- Cyganowski, C.J., Brogan, C.L., Hunter, T.R., Churchwell, E.: 2009, *ApJ* 702, 1615
- Ellingsen, S.P.: 2007, *MNRAS* 377, 571
- Ellingsen, S.P., von Bibra, M.L., McCulloch, P.M., Norris, R.P., Deshpande, A.A., Phillips, C.J.: 1996, *MNRAS* 280, 378
- Etoka, S., Cohen, R.J., Gray, M.D.: 2005, *MNRAS* 360, 116
- Gaylard, M.J., MacLeod, G.C.: 1993, *MNRAS* 262, 43
- Goddi, C., Moscadelli, L., Sanna, A., Cesaroni, R., Minier, V.: 2007, *A&A* 461, 1027
- Goedhart, S., Gaylard, M.J., van der Walt, D.J.: 2004, *MNRAS* 355, 553
- Green, J.A., Caswell, J.L., Fuller, G.A., et al.: 2009, *MNRAS* 392, 783
- Green, J.A., Caswell, J.L., Fuller, G.A., et al.: 2010, *MNRAS* 409, 913
- Harvey-Smith, L., Soria-Ruiz, R., Duarte-Cabral, A., Cohen, R.J.: 2008, *MNRAS* 384, 719
- MacLeod, G.C., Gaylard, M.J.: 1992, *MNRAS* 256, 519
- Malyshev, A.V., Sobolev, A.M.: 2003, *A&AT* 22, 1
- Menten, K.M.: 1991, *ApJ* 380, L75
- Minier, V., Booth, R.S., Conway, J.E.: 2000, *A&A* 362, 1093
- Minier, V., Conway, J.E., Booth, R.S.: 2001, *A&A* 369, 278
- Minier, V., Ellingsen, S.P., Norris, R.P., Booth, R.S.: 2003, *A&A* 403, 1095
- Moscadelli, L., Goddi, C., Cesaroni, R., Beltrán, M.T., Furuya, R.S.: 2007, *A&A* 472, 867
- Ott, M., Witzel, A., Quirrenbach, A., Krichbaum, T.P., Standke, K.J., Schalinski, C.J., Hummel, C.A.: 1994, *A&A*, 284, 331
- Pandian, J.D., Goldsmith, P.F.: 2007, *ApJ* 699, 435
- Pandian, J.D., Goldsmith, P.F., Deshpande, A.A.: 2007, *ApJ* 656, 255
- Pandian, J.D., Momjian, E., Xu, Y., Menten, K.M., Goldsmith, P.F.: 2011, *ApJ* 730, 55
- Pestalozzi, M.R., Minier, V., Booth, R.S.: 2005, *A&A* 432, 737
- Reid, M.J., Menten, K.M., Zheng, X.W., et al.: 2009, *ApJ* 700, 137
- Rygl, K.L.J., Brunthaler, A., Reid, M.J., Menten, K.M., van Langevelde, H.J., Xu, Y.: 2010, *A&A* 511, A2
- Sanna, A., Moscadelli, L., Cesaroni, R., Tarchi, A., Furuya, R.S., Goddi, C.: 2010, *A&A* 517, 78
- Schutte, A.J., van der Walt, D.J., Gaylard, M.J., MacLeod, G.C.: 1993, *MNRAS* 261, 783
- Slysh, V., Val'ts, I., Kalenskii, S.: 1999, *A&AS* 134, 115
- Sridharan, T.K., Beuther, H., Schilke, P., Menten, K.M., Wyrowski, F.: 2002, *ApJ* 566, 931
- Sugiyama, K., Fujisawa, K., Doi, A., Honma, M., Isono, Y., Kobayashi, H., Mochizuki, N., Murata, Y.: 2008, *PASJ* 60, 23
- Szymczak, M., Hrynek, G., Kus, A.: 2000, *A&AS* 143, 269
- Szymczak, M., Kus, A., Hrynek, G., Kepa, A., Pazderski, E.: 2002, *A&A* 392, 277
- Szymczak, M., Wolak, P., Bartkiewicz, A., van Langevelde, H.J.: 2011, *A&A* 531, L3
- van der Walt, D.J., Gaylard, M.J., MacLeod, G.C.: 1995, *A&AS* 110, 81
- van der Walt, D.J., Retief, S.J.P., Gaylard, M.J., MacLeod, G.C.: 1996, *MNRAS* 282, 1085
- Walsh, A.J., Hylard, A.R., Robinson, G., Burton, M.G.: 1997, *MNRAS* 291, 261
- Walsh, A.J., Burton, M.G., Hyland, A.R., Robinson G.: 1998, *MNRAS* 301, 640
- Xu, Y., Zheng, X.-W., Jiang, D.-R.: 2003, *Chinese J. A&A* 3, 49
- Xu, Y., Li, J.J., Hachisuka, K., Pandian, J.D., Menten, K.M., Henkel, C.: 2008, *A&A* 485, 729
- Xu, Y., Voronkov, M.A., Pandian, J.D., et al.: 2009, *A&A* 507, 1117